



Synthesis and HDAC inhibitory activity of isosteric thiazoline-oxazole largazole analogs



Jennifer M. Guerra-Bubb^a, Albert A. Bowers^a, William B. Smith^d, Ronald Paranal^d, Guillermina Estiu^c, Olaf Wiest^c, James E. Bradner^d, Robert M. Williams^{a,b,*}

^a Department of Chemistry, Colorado State University, Fort Collins, CO 80523, United States

^b University of Colorado Cancer Center, Aurora, CO 80045, United States

^c Department of Chemistry & Biochemistry, University of Notre Dame, Notre Dame, IN 46556, United States

^d Department of Medical Oncology, Dana-Farber Cancer Institute, Boston, MA 02115, United States

ARTICLE INFO

Article history:

Received 4 May 2013

Accepted 3 June 2013

Available online 18 June 2013

Keywords:

Largazole

HDAC

Oxazole

Isostere

Conformation

ABSTRACT

The synthesis of an isosteric analog of the natural product and HDAC inhibitor largazole is described. The sulfur atom in the thiazole ring of the natural product has been replaced with an oxygen atom, constituting an oxazole ring. The biochemical activity and cytotoxicity of this species is described.

© 2013 Elsevier Ltd. All rights reserved.

Largazole, isolated in 2008 by Luesch and coworkers,^{1,2} has been heavily studied as a possible candidate for cancer therapeutics. Largazole has emerged as one of the most potent histone deacetylase inhibitors (HDACi's) and is constituted of the sulfur-containing 3-hydroxy-7-mercaptohept-4-enoic acid moiety common to several other macrocyclic depsipeptide natural products including FK228 (romidepsin), FR901375 and the spiruchostatins. While the zinc-dependent, Class I hydrolases (HDACs 1, 2, 3 and 8) are implicated in malignant transformation, Class II hydrolases (HDACs 4–7, 9 and 10) mainly appear to be involved in the regulation of differentiation, such as myogenesis, neuronal differentiation and osteogenesis.³ The Class IIa HDAC's have been reported to compete with the histone acetyl transferase for direct binding to MEF2, perhaps modulating myocyte differentiation. Alternatively, the Class IIb enzyme HDAC6, which is a cytoplasmic-localized and cytoskeleton-associated deacetylase, is required for efficient oncogenic transformation and tumor formation.³

The pharmacophore model for HDAC inhibition contains three elements, namely: (1) a surface recognition unit which interacts with the opening to active site on the surface of the HDAC protein; (2) a metal-binding domain which serves to coordinate to the active site zinc ion and; (3) a linker connecting the surface recognition domain to the zinc-binding arm.^{4,5} To date, there are several

known natural and synthetic HDAC inhibitors, all of which have different variations of the three core elements, a representative sampling of which are depicted in Figure 1.⁶

Our group has previously disclosed a scalable total synthesis of largazole, which displays sub-nanomolar inhibitory activity against HDACs 1, 2 and 3. The synthetic approach that we developed for the synthesis of largazole has also been applied to the synthesis of various analogs of both FK228 and largazole.⁷

As part of a program directed at improving the isoform selectivity and drug-like properties of HDACi's based on the largazole molecular scaffold, we report herein the synthesis, modeling and biological activity of largazole analogs containing a single-atom substitution of the sulfur atom in the largazole thiazole for an oxygen atom making the corresponding oxazole.

The synthetic approach to this analog is based on the synthetic sequence previously used by our group in generating numerous other largazole analogs. The thiazoline-oxazole fragment (**2**) was constructed starting from known oxazole **1** (Scheme 1).⁷ Conversion of **1** into the corresponding nitrile proceeded via a two-pot procedure wherein **1** was first treated with NH₄OH in MeOH, then POCl₃ with Et₃N in dichloromethane. The crude nitrile was then condensed with α -methyl cysteine to provide the thiazoline-oxazole fragment (**2**) in 76% yield over three steps.

The heptenoic acid fragment (**6**), previously published by our group,⁸ was made starting from acrolein (**3**, Scheme 2). A Michael addition, followed by a Wittig reaction with commercially

* Corresponding author. Tel.: +1 9704916747.

E-mail address: robertmwilliams8@gmail.com (R.M. Williams).

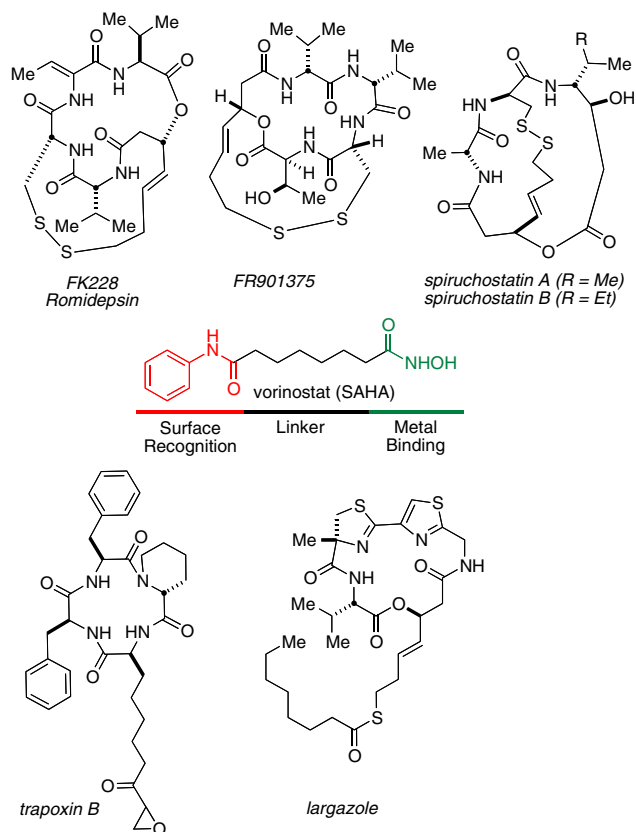
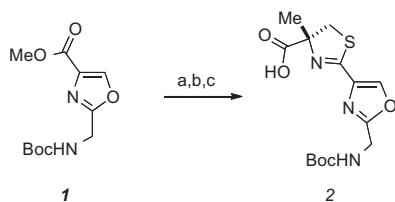


Figure 1. Selected natural and synthetic HDAC inhibitors.



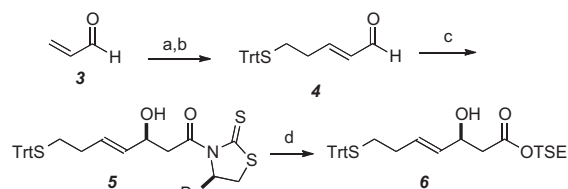
Scheme 1. Reagents: (a) NH_4OH , MeOH; (b) POCl_3 , Et_3N , CH_2Cl_2 ; (c) α -Me-Ser-OH•HCl, Et_3N , MeOH.

available (formylmethylene)triphenyl phosphorane, gave the α,β -unsaturated aldehyde (**4**). An aldol reaction utilizing a Crimmins auxiliary provided the β -hydroxy acid (**5**) and the chiral auxiliary was then displaced with trimethylsilyl ethanol to give the requisite coupling fragment (**6**).⁸

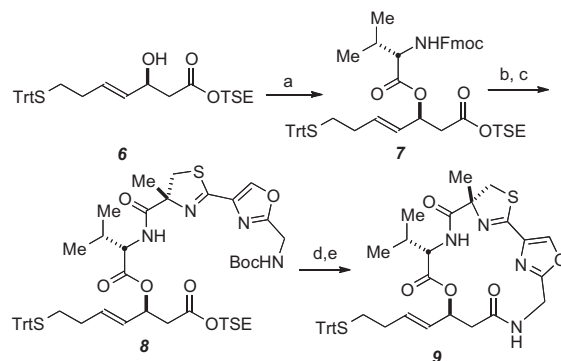
Construction of the macrocycle began with coupling the β -hydroxy acid (**6**) to N-Fmoc-Val-OH with EDCI, and Hunig's base, giving peptide **7** (Scheme 3).⁸ Deprotection followed by coupling of the thiazoline-oxazole (**2**) fragment with PyBOP and Hunigs base gave the desired substrate (**8**) in 91% yield over the two steps.⁷

The macrocyclization had initially been performed in our group via a HATU/HOBt coupling protocol,⁸ but due to vast amounts of the common HATU by-product tetramethylurea, and the difficulties to purify the reaction, another approach was investigated for the macrocyclization to render the purification step more amenable. Following a one-pot double-deprotection of **8** to the corresponding amino acid, the desired macrocycle (**9**) was obtained in 30% yield using T3P and Hunigs base.

Removal of the S-trityl residue of the macrocycle (**9**) with TFA and $i\text{Pr}_3\text{SiH}$ ⁸ in degassed dichloromethane gave, instead of the



Scheme 2. Reagents and compounds: (a) TrtSH, Et_3N , CH_2Cl_2 ; (b) (formylmethylene)triphenylphosphorane, PhH, 80 °C, 62%; (c) (*R*)-1-(4-benzyl-2-thioxothiazolidin-3-yl)ethanone, TiCl_4 , DIPEA, CH_2Cl_2 , 56%; (d) 2-(trimethylsilyl)ethanol, imidazole, CH_2Cl_2 .

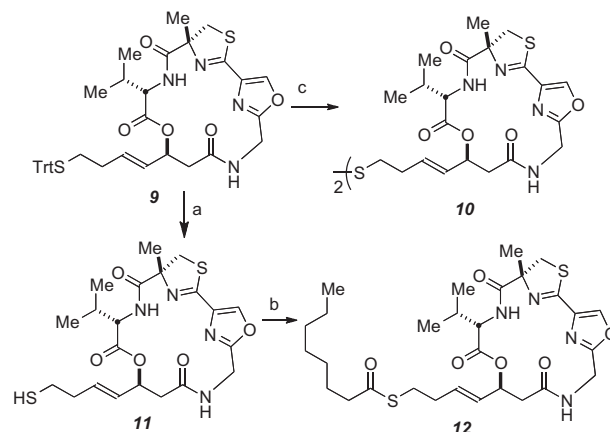


Scheme 3. Reagents and compounds: (a) N-Fmoc-Val-OH, EDCI, DIPEA, CH_2Cl_2 , 65%; (b) Et_2NH , CH_3CN ; (c) PyBOP, DIPEA, **2**, CH_2Cl_2 , 91%; (d) $\text{CF}_3\text{CO}_2\text{H}$, CH_2Cl_2 ; (e) T3P, DIPEA, CH_2Cl_2 , 30%.

expected thiol, the homo-dimeric disulfide product (**10**) in 35% yield (Scheme 4).

Interestingly, it was found that removal of the trityl residue of **9** with Et_3SiH instead of $i\text{Pr}_3\text{SiH}$ in degassed dichloromethane gave the desired thiol (**11**), which was immediately acylated to give the desired octanoyl-thioester (**12**).

To investigate the mode of binding of the isosteric analog to different HDAC isoforms, we used the previously described⁹ protocol of docking followed by 30 ns molecular dynamics simulations to study the binding of the thiol **11** to HDAC1 as well as the Class IIb HDAC6, which was not studied previously. The structure obtained for **11** bound to HDAC1 closely resembles the one of largazole.¹⁰ We have shown previously that the isoform selectivity of different HDAC inhibitors depends among other factors on the



Scheme 4. Reagents and compounds: (a) $\text{CF}_3\text{CO}_2\text{H}$, Et_3SiH , CH_2Cl_2 , 83%; (b) octanoylchloride, Et_3N , CH_2Cl_2 , 36%; (c) $\text{CF}_3\text{CO}_2\text{H}$, $i\text{Pr}_3\text{SiH}$, CH_2Cl_2 , 35%.

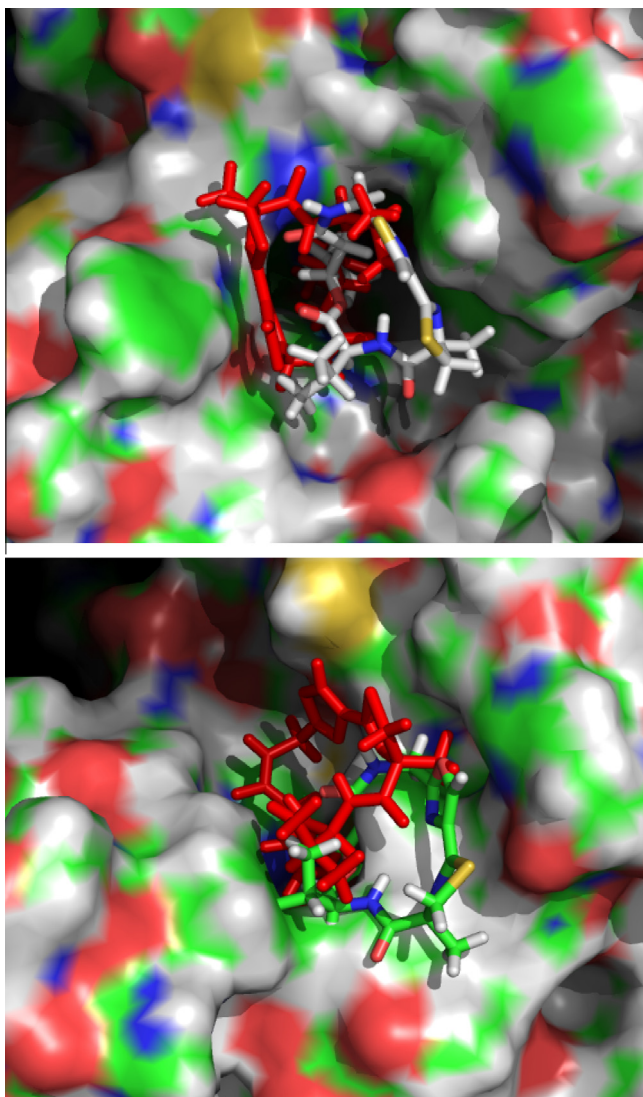


Figure 2. Structure of largazole thiol (top panel) and **11** bound to HDAC6 from MD simulations.

Table 1
HDAC activity of largazole analogs (IC₅₀ μM).

Compd	HDAC1	HDAC2	HDAC3	HDAC6	HDAC7	HDAC8
10	0.15	1.3	0.55	0.05	-	-
11	0.0044	0.020	0.0072	0.098	0.96	1.2
12	0.95	2.1	1.9	1.1	-	-
Largazole	0.23	0.90	0.67	0.34	-	-

interactions of the cap group with the protein and that the shape of the protein surface around the mouth of the binding site differs significantly between Class I and Class IIb HDACs.^{9,11}

Figure 2 shows largazole thiol (top panel) and **11** (bottom panel) bound to the mouth of the binding site in our previously described model of the C-terminal domain of HDAC6.⁹ Two binding conformations of similar energy that do not interconvert on the timescale of the MD simulation were found for both largazole and **11** (shown in atom colors and in red). Interestingly, the conformations found for **11** stacks against aromatic residues on opposite sides of the protein surface compared to the ones found for largazole thiol, possibly due to the differences in electronic character of the thiazole and the oxazole heterocycles. The shape complemen-

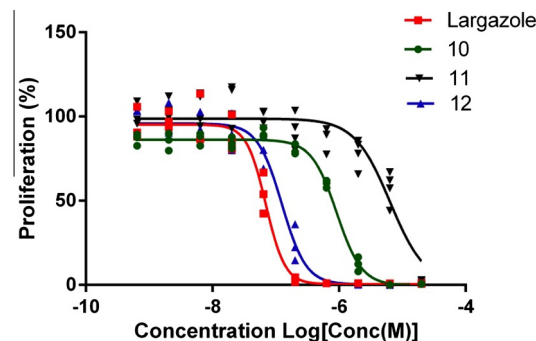


Figure 3. Activity of largazole analogs in MM1S cell line.

tarity of the cap group to the surface of HDAC6 is better than in the previously described model of largazole and HDAC1⁸ due to the larger, Y-shaped mouth of the binding site in HDAC6, resembling the case of tubacin.⁹ Nevertheless, the shape of the cap group only allows one of the two stacking interactions to occur at a given time, leading to the two possible orientations.

Compounds **10–12** were tested for inhibitory activity against HDACs 1–9, using an optimized homogenous assay performed in a 384-well plate, as described before.^{8,10} The results of these studies, summarized in Table 1, indicate that **11** is more active than the natural pro-drug largazole and similar in potency to the largazole thiol. Interestingly, **11** are also active in HDAC7 and HDAC8, albeit only at ~1 μM concentration, where neither of the other compounds showed appreciable activity. These studies demonstrate that the free thiol group is essential for activity. It should be noted that both Class IIa HDACs such as HDAC7, as well as HDAC8, are known to adopt multiple conformations which can result in large pockets around the binding sites¹¹ that would be well-suited for the binding of a large cap group such as the one of largazole thiol and its analogs.

Next, we tested the activity of the novel analogs in the MM1.S multiple myeloma cell line. As can be seen in Figure 3, **11** has an IC₅₀ of 6.2 μM significantly less active than in the biochemical assay, presumably due to degradation of the free thiol in the cellular environment. The prodrugs **10** and **12** displayed IC₅₀'s of 0.91 and 0.12 μM, which are comparable to largazole itself.

We have conscripted our robust synthetic strategy that we previously deployed for the synthesis of largazole and numerous analogs, to make a single-atom isosteric oxazole analog of the natural product. Two unexpected and potentially significant differences emerged from this study. First, the computational study revealed that **11**, binds to HDAC6 in a conformation that is quite distinct from that of largazole thiol. The underlying stereoelectronic bases for these remains an area worthy of further study and scrutiny. Secondly, the unexpected activity of the oxazole analog toward the Class IIb enzymes, compared to that of the natural product were quite unexpected, particularly as this single atom isosteric change would not a priori, be anticipated to lead to such biochemical reactivity differences. This reveals that subtle electronic properties within the cap group, can have profound effects on the conformational disposition and attendant biochemical and possibly biological activity of these highly potent HDACi's. The results recorded here, provide a powerful incentive for additional detailed exploration of seemingly small structural changes and stereoelectronic alterations in the cap groups of macrocyclic HDACi's, such as largazole, that might manifest as HDAC isoform-specific reactivity profile signatures. The complex interactions of the protein surface near the opening to the active site with these relatively conformationally rigid inhibitors is obviously an area ripe for exploitation and constitutes a major thrust of our ongoing efforts.

Acknowledgements

This work was supported by the National Institutes of Health (grant# RO1 CA152314, to RMW) and for a postdoctoral fellowship for AAB (NCI Grant CA136283). We also acknowledge financial support from the Colorado State University Cancer Supercluster. Mass Spectra were obtained on instruments supported by the NIH Shared Instrument Grant GM49631. We thank Ralph Mazitschek for the provision of acetylated substrate. JEB acknowledges support by grants from the National Cancer Institute (1K08CA128972) and the Burroughs-Wellcome Foundation (CAMS).

Supplementary data

Supplementary data (complete experimental details for the preparation of all new compounds and detailed description of biochemical and cellular assays as well as description of the computational studies) associated with this article can be found, in the online version, at <http://dx.doi.org/10.1016/j.bmcl.2013.06.012>.

References and notes

1. Taori, K.; Paul, V. J.; Luesch, H. *J. Am. Chem. Soc.* **2008**, *130*, 13506.
2. Ying, Y. C.; Taori, K.; Kim, H.; Hong, J. Y.; Luesch, H. *J. Am. Chem. Soc.* **2008**, *130*, 8455.
3. Aldana-Masangkay, G. I.; Sakamoto, K. M. *J. Biomed. Biotechnol.* **2011**, *2011*, 875824.
4. Jung, M.; Hoffmann, K.; Brosch, G.; Loidl, P. *Bioorg. Med. Chem. Lett.* **1997**, *7*, 1655.
5. Remiszewski, S. W.; Sambucetti, L. C.; Atadja, P.; Bair, K. W.; Cornell, W. D.; Green, M. A.; Howell, K. L.; Jung, M.; Kwon, P.; Trogani, N.; Walker, H. *J. Med. Chem.* **2002**, *45*, 753.
6. Newkirk, T. L.; Bowers, A. A.; Williams, R. M. *Nat. Prod. Rep.* **2009**, *26*, 1293.
7. Bowers, A. A.; West, N.; Newkirk, T. L.; Troutman-Youngman, A. E.; Schreiber, S. L.; Wiest, O.; Bradner, J. E.; Williams, R. M. *Org. Lett.* **2009**, *11*, 1301.
8. Bowers, A.; West, N.; Taunton, J.; Schreiber, S. L.; Bradner, J. E.; Williams, R. M. *J. Am. Chem. Soc.* **2008**, *130*, 11219.
9. Estiu, G.; Greenberg, E.; Harrison, C. B.; Kwiatkowski, N. P.; Mazitschek, R.; Bradner, J. E.; Wiest, O. *J. Med. Chem.* **2008**, *51*, 2898.
10. Bowers, A.; Greshock, T.; West, N.; Estiu, G.; Schreiber, S.; Wiest, O.; Williams, R.; Bradner, J. *J. Am. Chem. Soc.* **2009**, *131*, 2900.
11. Estiu, G.; West, N.; Mazitschek, R.; Greenberg, E.; Bradner, J.; Wiest, O. *Bioorg. Med. Chem.* **2010**, *18*, 4103.